

E6-2002-202

S. A. Kudrya\*, V. M. Gorozhankin, K. Ya. Gromov,  
Sh. R. Malikov, L. A. Malov, V. A. Sergienko\*,  
V. I. Fominykh, V. V. Tsupko-Sitnikov, V. G. Chumin,  
E. A. Yakushev

ALPHA DECAY  $^{225}\text{Ac} \rightarrow ^{221}\text{Fr}$

Submitted to «Известия РАН, серия физическая»

---

\*St. Petersburg State University, Russia

# I. Introduction

Considerable study has been given to nuclei with  $A = 220 - 230$  recently. In this region there occurs transition from the spherical to the deformed nuclear shape, which gives rise to some specific features in the nuclear structure. In particular, negative parity levels with low excitation energies have been found in even-even nuclei from this region [1]. These are, for example,  $I^\pi = 1^-$  levels with energy about 600 keV in radon nuclei and 200  $\div$  500 keV in radium and thorium nuclei. Presence of these states may point to reflection symmetry breaking in nuclei. Calculations allow a definite conclusion that these nuclei are soft in terms of octupole deformation  $\beta_3$ . However, as to presence of static octupole deformation in all nuclei from the region in question, opinions differ. For example, in [2, 3] the authors point to importance of  $\beta_3$  when considering negative parity states. Calculation of octupole vibrational states in thorium isotopes [4] were carried out under the assumption of their mirror symmetry ( $\beta_2 \neq 0$ ,  $\beta_4 \neq 0$ ,  $\beta_3 = 0$ ). Octupole states at the beginning of the actinide region were investigated [5] with allowance made for Coriolis mixing of rotational bands with different projections of the angular momentum  $K = 0, 1, 2, 3$  onto the symmetry axis of the nucleus. These calculations are in quite good agreement with the experimental data. In [6] the appearance of low-lying  $1^-$ -states is ascribed to softness of the nuclei in terms of the cluster mode of excitation and to manifestation of multiparticle cluster configurations in their structure. Thus, properties of low-lying states in nuclei from the atomic weight region in question, especially in odd  $A$  nuclei, are in general a rather complicated problem, which needs further investigation.

One of the nuclei allowing experimental investigation of the above properties is  $^{221}\text{Fr}$ . The nuclide  $^{221}\text{Fr}$  is from the region of isotopes which does not include stable nuclei and thus it cannot be studied in several-nucleon transfer reactions. In addition, the neutron excess in this nucleus makes it impossible to study the nucleus in reactions with heavy ions. Experimental information on the  $^{221}\text{Fr}$  level structure can only be gained from investigation of the  $^{225}\text{Ac}$  ( $T_{1/2} = 10$  days) alpha decay or the  $^{221}\text{Rn}$  ( $T_{1/2} = 25$  min) beta decay. In the latter case the possibilities of the investigation are restricted by difficulties in making of  $^{221}\text{Rn}$  sources. Therefore, most information on the structure and properties of  $^{221}\text{Fr}$  is derived from investigation of the  $^{225}\text{Ac}$   $\alpha$ -decay. The  $\alpha$ -particle spectrum from the  $^{225}\text{Ac}$  decay was investigated by Dzhelepov et al. [7] and Bastin-Scoffier [8]. The

data of both investigations on weak fine-structure lines are somewhat in conflict. Below we use the data on energies and intensities of  $\alpha$ -spectrum lines evaluated by Akovali [9]. The  $\gamma$ -ray spectrum was studied in a number of papers [10–12]. Recently the  $^{225}\text{Ac}$   $\alpha$ -spectrum has been studied by Kouassi et al. [13, 14] and Ardisson et al. [15]. Plenty of additional information on low-intensity  $\gamma$ -rays has been gained, but in some cases assignment of  $\gamma$ -rays to the  $^{225}\text{Ac}$  decay requires confirmation. To analyze the structure of excited states one should have information on multipolarity of  $\gamma$ -transitions and the internal conversion electron (ICE) spectrum. The best and virtually sole investigation of the  $^{225}\text{Ac}$  ICE spectrum is that by Dzhelepov et al. [16, 11]. Additional investigation of the ICE spectrum in the range 5 – 25 keV has recently been carried out by Yakushev et al. [17]. Liang et al. [18] have measured life-times of some excited levels in  $^{221}\text{Fr}$ . Peghaire [19] and Gromov et al. [20] studied coincidences of alpha particles with gamma rays at the  $^{225}\text{Ac}$  decay.

The purpose of the present paper is to refine the existing experimental data on the  $^{225}\text{Ac} \rightarrow ^{221}\text{Fr}$  decay and to get new ones. Emphasis is placed on investigation and quantitative analysis of ( $\alpha$ - $\gamma$ )-coincidences in order to prove that gamma transitions belong to the  $^{225}\text{Ac}$  decay and to place them in the  $^{221}\text{Fr}$  level scheme. The  $^{225}\text{Ac} \rightarrow ^{221}\text{Fr}$  decay scheme is constructed on the basis of the previously known and new experimental data.

## II. Experimental conditions

Gamma ray spectra and ( $\alpha$ - $\gamma$ )-coincidences were investigated at a facility described in [21]. Coincidence ( $E_\alpha$ ,  $E_\gamma$ ,  $t$ )-events were recorded in the computer memory in the in-list mode. Single  $\alpha$ - and  $\gamma$ -spectra were simultaneously recorded. Alpha particles were detected by a surface-barrier Si(Au) detector (diameter 10mm, FWHM 20–25 keV). To get better  $\alpha$ -particle efficiency (larger solid angle), ( $\alpha$ - $\gamma$ )-coincidences were studied in the short-range geometry: the distance between the  $\alpha$ -source and the detector was 1.5 – 2 cm. Therefore, the real experimental energy resolution for the  $\alpha$ -spectrum was 25 – 35 keV. Precise investigation of the  $\alpha$ -spectrum was not among our objectives because a semiconductor could hardly improve the results obtained with magnetic spectrographs [7, 8]. To detect gamma rays we used HPGe detectors of volume 2 cm<sup>3</sup> (FWHM – 0.8 keV at  $E_\gamma = 122$  keV), 84 cm<sup>3</sup> (FWHM – 1 keV at  $E_\gamma = 150$  keV), and

200 cm<sup>3</sup> (FWHM – 3.5 keV at  $E_\gamma = 1332$  keV). Energy and efficiency calibration of the  $\gamma$ -detectors was carried out with standard  $\gamma$ -sources (<sup>133</sup>Ba, <sup>134</sup>Cs, <sup>169</sup>Yb, and others). When sorting the ( $\alpha$ - $\gamma$ )-coincidence energy spectra, we took the window in the delayed coincidence time spectrum to be 100 ns.

<sup>225</sup>Ac ( $T_{1/2} = 10$  days) sources were separated from the <sup>229</sup>Th ( $T_{1/2} = 7340$  years) by " <sup>225</sup>Ac isotope generator" method [22]. <sup>229</sup>Th was separated from the reactor uranium bar more than 10 years before the beginning of the experiments. The separated <sup>225</sup>Ac was put on a tantalum foil and then was vacuum evaporated onto an aluminum foil. The activity of the sources was as high as 25 – 30  $\mu$ Ci. Short-lived <sup>225</sup>Ac daughter nuclides were accumulated in the sources. No another impurities were observed in the sources.

### III. Experimental results

#### 1. <sup>225</sup>Ac $\gamma$ -ray spectrum

Investigation of the <sup>225</sup>Ac decay  $\gamma$ -spectrum faces a difficulty arising from presence of other <sup>225</sup>Ac decay chain members in the <sup>225</sup>Ac sources. With  $\gamma$ -rays from the decays <sup>221</sup>Fr ( $T_{1/2} = 4.8$  min), <sup>217</sup>At (32 ms), <sup>213</sup>Bi (46 min), and <sup>209</sup>Tl (2.2 min) appearing in the spectrum, it is difficult to observe low-intensity  $\gamma$ -transitions and to identify them with the <sup>225</sup>Ac decay. To remove  $\gamma$ -rays of daughter isotopes and  $\gamma$ -rays of the natural background from the <sup>225</sup>Ac spectrum, we analyzed as a single <sup>225</sup>Ac  $\gamma$ -spectrum the spectrum of  $\gamma$ -rays coinciding with  $\alpha$ -particles in the energy interval  $E_\alpha = 4,5 \div 5,8$  MeV. This interval fully covers the <sup>225</sup>Ac  $\alpha$ -spectrum [7, 8] and only partially the <sup>221</sup>Fr  $\alpha$ -spectrum. <sup>213</sup>Bi  $\alpha$ -particles with  $E_\alpha = 5.55$  MeV also fall within the  $E_\alpha = 4,5 - 5,8$  MeV interval. Consequently, 218.0, 359.9, and 538.0-keV  $\gamma$ -rays from the <sup>221</sup>Fr decay and 323.8-keV  $\gamma$ -rays from the <sup>213</sup>Bi are observed in the coincidence spectrum for  $E_\alpha = 4.5-5.8$  MeV. By studying  $\gamma$ -spectra coinciding with  $\alpha$ -particles in narrow  $\alpha$ -energy intervals we determined energies of  $\alpha$ -particles coinciding with these  $\gamma$ -transitions and found that the above-mentioned  $\gamma$ -transitions could not occur at the <sup>225</sup>Ac decay. Analyzing the <sup>225</sup>Ac  $\gamma$ -spectrum we also used the results from our investigations of the <sup>221</sup>Fr [23], <sup>217</sup>At [24, 25], <sup>213</sup>Bi, and <sup>209</sup>Tl decays [26, 27]. Confining the list of <sup>225</sup>Ac  $\gamma$ -rays to transitions observed in ( $\alpha$ - $\gamma$ )-coincidences, we may, of course, overlook  $\gamma$ -rays arising

from the decay of isomeric  $^{221}\text{Fr}$  states with lifetimes larger than the time window width 100 ns. Isomeric states like this are not known. In [18] lifetimes of a few  $^{221}\text{Fr}$  levels were measured. They are all smaller than one nanosecond.

Intensities of  $^{225}\text{Ac}$   $\gamma$ -rays in per cent of decay are calculated from the analysis of the  $\gamma$ -ray spectrum of the equilibrium  $^{225}\text{Ac}$  chain decay in relation to the intensity of 218.0-keV  $\gamma$ -rays from the  $^{221}\text{Fr}$   $\alpha$ -decay. The 218.0-keV  $\gamma$ -ray intensity equal to 11.2% of decays is found from the intensity of the  $^{221}\text{Fr}$   $\alpha$ -decay to the  $^{217}\text{At}$  level at 218.0 keV,  $I_{\alpha 218} = 15.3(3)\%$  [7], and the theoretical total conversion coefficient of the 218.0-keV  $\gamma$ -transition. The multipolarity of the 218.0-keV  $\gamma$ -transition, E2, was established by Dzhelepov et al. [16].

In Table 1 the  $^{225}\text{Ac}$   $\gamma$ -ray spectrum data gained by us are compared with the latest results of Ardisson et al. [15]. Intensities of relatively stronger gamma rays usually agree within the double error. We consider this agreement satisfactory. Considerable disagreement is observed between intensities of the 99.6 and 99.8-keV, 73.5 and 73.8-keV  $\gamma$ -rays. We calculated gamma ray intensities of these two doublets using the data of Dzhelepov et al. [11] on the conversion electron spectrum because we do not think that decomposition of these complex peak in our gamma spectrum is reliable. We ascribe to the  $^{225}\text{Ac}$  decay 21 new gamma transitions not observed in [15]. We do not observe 18 gamma transitions ascribed to the  $^{225}\text{Ac}$  decay in [15]. Some of them were assigned to the  $^{225}\text{Ac}$  by mistake. For example, the measured energy of  $\alpha$ -particles coinciding with 809.3-keV gamma rays makes it possible to reliably identify the observed coincidences with the  $^{221}\text{Fr}$   $\alpha$ -decay to the earlier unknown  $^{217}\text{At}$  level at 809.3 keV [28]. The 446.31, 656.18, 657.88, and 667.10-keV gamma rays are also identified with the  $^{221}\text{Fr}$  decay [23]. The last column of the table indicates placement of  $\gamma$ -transitions in the  $^{221}\text{Fr}$  level scheme: absence of parentheses means that the placement is reliably confirmed by ( $\alpha$ - $\gamma$ )-coincidences, parentheses mean that ( $\alpha$ - $\gamma$ )-coincidences are not in conflict with the placement.

## 2. $^{221}\text{Fr}$ level scheme

To establish the position of a  $\gamma$ -transition in the  $^{221}\text{Fr}$  level scheme, the results of ( $\alpha$ - $\gamma$ )-coincidence investigations were analyzed as follows. The  $^{225}\text{Ac}$   $\alpha$ -spectrum ( $E_{\alpha} = 4.5 - 5.8$  MeV) was divided into equal regions

25 keV long. A spectrum of  $\gamma$ -rays coinciding with  $\alpha$ -particles falling within each energy region was produced (sorted out). Then dependences the peak areas  $S_{\gamma ik}^\alpha(E_\alpha)$  on the energies of  $\alpha$ -particles were constructed for all  $\gamma$ -transitions presented in Table 1. Obviously, for  $\gamma$ -rays from the same level these dependences should be similar: energies  $E_\alpha$  and ratios of  $\alpha$ -peak areas must be equal. The peak with the largest energy  $E_\alpha$  corresponds to the  $\alpha$ -decay to the level from which the transition  $\gamma_{ik}$  in question proceeds. Peaks with smaller  $E_\alpha$  appear when level  $i$  is noticeably populated from higher levels through cascade  $\gamma$ -transitions. Figure 1 displays  $S_{\gamma ik}^\alpha(E_\alpha)$  plots for the 224.7, 198.4, 188.0, 124.8, and 123.8-keV  $\gamma$ -transitions. A maximum at  $E_\alpha = 5600(15)$  keV is observed for all these  $\gamma$ -transitions. The energy of the group of  $\alpha$ -particles measured with magnetic spectrographs is  $E_{\alpha 224.6} = 5609(3)$  keV, i.e., all five  $\gamma$ -transitions proceed from the same level of 224.6 keV. No other maxima are observed in the  $S_{\gamma ik}^\alpha(E_\alpha)$  plots (Fig. 1); thus, no noticeable population of the 224.6-keV level from higher levels occurs. Figure 2 displays the function  $S_{\gamma 108,3}^\alpha(E_\alpha)$ . Apart from the maximum at ( $E_\alpha = 5720(15)$  keV corresponding to the  $\alpha$ -decay to the level at 108.3 keV (magnetic  $E_\alpha$  is 5724(3) keV), we observe maxima of coincidences at  $\alpha$ -particle energies 5628(15), 5575(15), 5442(15), and 5296(30) keV indicating population of the 108.3-keV level from the levels at 195.8, 253.5, 393.2, and  $\sim 600$  keV. The  $S_{\gamma 179,8}^\alpha$  and  $S_{\gamma 249,6}^\alpha$  plots (Fig. 3) show that the level at 288.1 keV ( $E_{\alpha magn.} = 5545(4)$  keV) is intensively populated from the level at 400.7 keV ( $E_{\alpha magn.} = 5436(4)$  keV). All  $\gamma$ -transitions from Table 1 were analyzed in this way. All placements of the  $\gamma$ -transitions in the  $^{221}\text{Fr}$  level scheme given in the table (without parentheses) are reliably proved.

For five  $\gamma$ -transitions (marked with the letter c in Table 1) it was impossible to infer definitely their place in the  $^{221}\text{Fr}$  level scheme though energies of  $\alpha$ -particles with which they coincide are found. For example, the energy of the  $\alpha$ -particles with which the  $\gamma$ -rays coincide suggested that the  $\gamma$ -transition of 173.40(10) keV proceeded from the level of 195.8 or 224.6 keV, the  $\gamma$ -transition of 183.00(10) keV from the level of 224.6 or 234.5 keV, the  $\gamma$ -transition of 193.20(10) keV from the level of 393.2 or 400.7 keV, the  $\gamma$ -transition of 231.3 keV from the level of 253.5 or 279.2 keV, and the  $\gamma$ -transition of 348.2 keV from the level of 393.2 or 400.7 keV. The calculated energies of the levels to which these  $\gamma$ -transitions proceed are not equal to the energies of the known levels. Three of these differences are 51.80(11) keV and two are 22.3(3) keV. Thus, we may assume that  $^{221}\text{Fr}$

has levels at 51.8(1) and 22.3(3) keV. However, we think that more data are necessary to introduce these levels. In addition, we cannot rule out a possibility that these low-intensity  $\gamma$ -transitions arise from the decay of other nuclides in the equilibrium  $^{225}\text{Ac}$  decay chain, first of all from the  $^{213}\text{Bi}$  decay. In [25] investigation of the  $^{213}\text{Bi}$   $\alpha$ -spectrum revealed that the intensity of fine-structure lines with energies below  $E_{\alpha 323,8} = 5549$  keV, if they exist, is no higher than 0.01% per decay. Intensities of the  $\gamma$ -rays in question are lower than or equal to  $\sim 0.01\%$  per decay, i.e. these  $\gamma$ -rays arise from the  $^{213}\text{Bi}$  decay should not be ruled out, though in all cases new energy levels have to be introduced in the  $^{213}\text{Bi} \rightarrow ^{209}\text{Tl}$  decay.

Placement of the 317.4-keV  $\gamma$ -transition also entailed problems. It was observed to coincide with  $\alpha$ -particles corresponding to population of the levels at (552.0–570.8) and 637.5 keV. In all cases coincidence areas were small. In the case of coincidence with  $E_{\alpha 637,5}$  it is necessary to introduce a level at 320 keV, which manifested itself only in the investigation of the  $\alpha$ -spectra. Therefore we think that the 317.4-keV transition most probably proceeds from the 552.0-keV level to the 234.5-keV level (transition multipolarity E1) and/or from the 570.8-keV level to the 253.5-keV level (transition multipolarity M1). In both cases multipolarity was inferred from the data on parities of the levels between which the transition occurs. We do not rule out a possibility that there exist two  $\gamma$ -transitions close in energy (about 317 keV).

The  $^{225}\text{Ac} \rightarrow ^{221}\text{Fr}$  decay scheme constructed on the basis of the ( $\alpha$ - $\gamma$ )-coincidence investigations and  $^{225}\text{Ac}$  gamma spectrum data is displayed in Fig. 4. It includes 31 excited states of the  $^{221}\text{Fr}$  nucleus. In [7, 8] the authors reported observation of over 40 fine-structure lines in the  $^{225}\text{Ac}$   $\alpha$ -spectrum, i.e., excitation of over 40 energy levels in  $^{221}\text{Fr}$ .

Fine-structure line intensities associated with the decay to levels not observed by us in ( $\alpha$ - $\gamma$ )-coincidences are small and data on them in [7, 8] are sometimes contradictory. Yet, we believe that some of these levels must be observed in ( $\alpha$ - $\gamma$ )-coincidences, e.g., levels at 310 keV ( $I_{\alpha} = 0,07(3)\%$ ), 349 keV ( $I_{\alpha} = 0,0020(7)\%$ ), 423 keV ( $I_{\alpha} = 0,0020(5)\%$ ), 680 keV ( $I_{\alpha} = 0,0020(8)\%$ ) and 943 keV ( $I_{\alpha} = 0,0020(5)\%$ ). The cause of not observing them in ( $\alpha$ - $\gamma$ )-coincidences may be either that their lifetimes are larger than the width of the time window used by us for analyzing ( $\alpha$ - $\gamma$ )-coincidences or that the corresponding  $\alpha$ -lines were ascribed to the  $^{225}\text{Ac}$  decay in [7, 8] by mistake. The experimental data do not confirm the levels at 271.1, 311.4, 320.04, 338.3, 348.3, 406.7, 422.6, 446.3, 482.0, 645.9, 679.4,

766.5, 808.5, and 942.8 keV introduced by Ardisson et al. [15]. We either do not observe gamma rays ascribed in [15] to de-excitation and population of these levels or the measured energies of the alpha particles coinciding with the gamma rays do not allow them to be ascribed to the  $^{225}\text{Ac}$  decay.

### 3. $^{221}\text{Fr}$ level populations by the $^{225}\text{Ac}$ $\alpha$ -decay

Investigations of ( $\alpha$ - $\gamma$ )-coincidences allow quite simple determination of the ratio between the intensity of the direct filling of a level by the  $\alpha$ -decay and the total population of the level—total intensity of all nuclear transitions to or from this level. A method of qualitative processing of the experimental data on coincidences of nuclear transitions [29] with using ratios of peak areas in the coincidence spectra and in single spectra was used. The area of the peak of coincidences of  $\gamma$ -rays from level  $i$  with the  $\alpha$ -particles of the  $\alpha$ -transition to level  $i$  is

$$S_{\gamma ik}^{\alpha i} = N \cdot ((a_{\alpha i} a_{\gamma ik}) / a_i) \cdot \varepsilon_{\alpha i} \cdot \varepsilon_{\gamma ik}$$

where  $N$  is the number of decays of the nuclide during the experiment,  $a_{\alpha i}$  is the intensity of the  $\alpha$ -transition to level  $i$ ,  $a_{\gamma ik}$  is the intensity of  $\gamma$ -rays from level  $i$  to level  $k$ ,  $a_i$  is total intensity of all nuclear transitions through level  $i$  (from here on the letter  $a$  denotes intensities of nuclear transitions in % of decays),  $\varepsilon_{\alpha i}$  and  $\varepsilon_{\gamma ik}$  are detection efficiencies for  $\alpha$ -particles and  $\gamma_{ik}$  quanta.

The area of the  $\gamma_{ik}$  peak in a single  $\gamma$ -spectrum is

$$S_{\gamma ik} = N \cdot a_{\gamma ik} \cdot \varepsilon_{\gamma ik} .$$

Calculating  $S_{\gamma ik}^{\alpha i} / S_{\gamma ik} = (a_{\alpha i} / a_i) \cdot \varepsilon_{\alpha i}$  and setting  $\varepsilon_{\alpha i} = \text{const}$ , we get ratios between the intensity of the direct population of a level by the  $\alpha$ -decay and the total intensity of population of level  $i$ ,  $a_{\alpha i} / a_i$ . The error of the result depends only on errors in determination of  $S_{\gamma ik}^{\alpha i}$  and  $S_{\gamma ik}$  and does not depend on the error in determination of the  $\gamma$ -ray detection efficiency. The calculated ratios  $a_{\alpha i} / a_i$  are presented in Table 2. They are seen to be determined quite accurately, in some cases the determination error is 2–4%. Note that for some higher levels, e.g., at 570.8, 602.3, 630.6 keV,  $a_{\alpha i} / a_i < 1$ . It might seem that  $a_{\alpha i} / a_i$  for high levels should be equal to unity because the  $\alpha$ -decay to higher levels is unlikely and, being of low energy,  $\gamma$ -transitions between high levels could not compete



with transitions from high levels to low-energy ones. However, it should be born in mind that density of levels increases with increasing energy of levels and  $\alpha$ -decay to them is possible, though with an extremely small, experimentally unobservable probability. Low-intensity  $\gamma$ -transitions from these levels to lower-lying ones may occur. The contribution from these  $\gamma$ -transitions to the level population will be more noticeable for levels the direct  $\alpha$ -decay to which is of low intensity.

The  $a_{\alpha i}/a_i$  values were used to calculate intensities of level population by the  $\alpha$ -decay,  $a_{\alpha i} = (a_{\alpha i}/a_i) a_i$ . For  $a_i$  we took the sum of total (including conversion) intensities of  $\gamma$ -transitions from a level. The calculated  $a_{\alpha i}$  (column 4 in Table 2) were compared with Akovali's [9] averaged  $a_{\alpha i}$  values derived from magnetic measurements. Values of  $a_{\alpha i}$  agree within the error for most groups of  $\alpha$ -particles, but error of  $a_{\alpha i}$  values found by us is smaller. The intensity of the  $\alpha$ -decay to the 145.9-keV level  $a_{\alpha 145,9} = 0,023(2)\%$  is found for the first time.

#### 4. Total intensities and multiplicities of $\gamma$ -transitions

Observation of coincidences not only with  $\alpha$ -particles populating level  $i$  but also with  $\alpha$ -particles populating higher levels  $p$  ( $E_{\alpha p} < E_{\alpha i}$ ) (see, for example, Fig. 2 and 3) in some spectra  $S_{\gamma ik}^{\alpha}(E_{\alpha})$  makes it possible to find the total intensity of the  $\gamma$ -transition from level  $p$  to level  $i$ . The area of the peak of coincidences of  $\gamma_{ik}$  rays with  $\alpha$ -particles filling level  $p$  is

$$S_{\gamma ik}^{\alpha p} = N \cdot ((a_{\alpha p} \cdot a_{pi} \cdot a_{\gamma ik}) / a_p \cdot a_i) \cdot \varepsilon_{\alpha i} \cdot \varepsilon_{\gamma ik},$$

where  $a_{pi}$  is the total (including conversion) intensity of the  $\gamma$ -transition(s) between levels  $p$  and  $i$ . The area of the peak of coincidences of  $\gamma_{ik}$  rays with  $\alpha$ -particles populating level  $i$  is

$$S_{\gamma ik}^{\alpha i} = N \cdot ((a_{\alpha i} \cdot a_{\gamma ik}) / a_i) \cdot \varepsilon_{\alpha i} \cdot \varepsilon_{\gamma ik}.$$

Using the ratio of these areas, we find the total  $\gamma$ -transition intensity  $a_{pi}$ :

$$a_{pi} = ((a_{\alpha i} \cdot a_p) / a_{\alpha p}) \cdot S_{\gamma ik}^{\alpha p} / S_{\gamma ik}^{\alpha i}.$$

To determine total  $\gamma$ -transition intensities, we took the cases where only one transition occurs between levels  $p$  and  $i$  (no cascades) and where the  $\alpha$ -spectrum resolution allows reliable determination of the peak areas  $S_{\gamma ik}^{\alpha p}$  and  $S_{\gamma ik}^{\alpha i}$ . Calculations were carried out with  $a_{\alpha p}/a_p$  and  $a_{\alpha i}$  from Table 2. Knowing the total intensity of the  $p \rightarrow i$   $\gamma$ -transition, we find the total internal conversion coefficient of the  $\gamma$ -transition  $\alpha_{\Pi pi} = (a_{pi}/a_{\gamma pi}) - 1$ . Values of  $a_{\gamma pi}$  are taken from Table 1. Comparing the results with the calculations [30] for different multipoles we infer the multipolarity ( $\sigma L$ ) of the  $\gamma$ -transition. The resulting total intensities and total internal conversion coefficients for seven  $\gamma$ -transitions are presented in Table 3. Multipolarities of five low-intensity  $\gamma$ -transitions are found for the first time. The inferred  $\sigma L$  of the 87.4 and 145.2-keV  $\gamma$ -transitions agree with the results of investigations of internal conversion electron spectra at the magnetic  $\beta$ -spectrometer [31, 16, 11]. All known multipolarities of  $\gamma$ -transitions at the  $^{225}\text{Ac}$  decay are given in column 5 of Table 1.

Note that when analyzing data on conversion electrons [11] of the 73.5 and 73.8, 99.6 and 99.8-keV  $\gamma$ -transitions together with our data on in-

tensities of  $\gamma$ -rays in these doublets (see Table 1), we found total intensities of the 73.9 and 99.8-keV  $\gamma$ -transitions, 0.30(2)% and 1.31(14)% respectively, and calculated their total internal conversion coefficients, 0.15(4) and 0.31(10) respectively. Comparison of these values with the theoretical ones confirms the conclusion [11] that these transitions are of E1 type with the M2 admixture less than 0.1% and 0.5%. For the 99.8-keV transitions this admixture is definitely no less than 0.3%, i.e., this E1 transition does have M2 admixture.

We analyzed data on conversion electrons from the  $^{225}\text{Ac} \rightarrow ^{221}\text{Fr}$  decay unidentified in [16, 31]. The conversion electrons with energies  $E_e = 95.5$  and 96.1 keV were interpreted as  $L_1$  and  $L_2$  lines of the earlier unknown 114-keV transition. The multipolarity of the  $E_{\gamma 114}$  transition found from the intensity ratio  $L_1: L_2, - M1 + (19 \pm 9\%)E2$ , agrees with the value found above from the total internal conversion coefficient (Table 3).

## 5. Internal conversion electron spectrum in the region 5.5–24 keV

Analyzing the transition intensity balance on the 26.0 and 36.7-keV levels, Dzhelepov et al. [31, 32] assumed existence of 10.6-keV  $\gamma$ -transition from the level at 36.7 keV to the level at 26.0 keV. To find this gamma transition and to refine, if possible, intensities of internal conversion electrons (ICE) of the 26.0, 36.7, and 38.5-keV  $\gamma$ -transitions, the spectrum of electrons from the  $^{225}\text{Ac}$  decay was investigated at an electrostatic spectrometer ISA-50 [17] with the instrumental energy resolution of 20 eV. As in the ( $\alpha$ - $\gamma$ )-experiments, the source was made by vacuum evaporation. In Table 4 the energies and intensities of ICE lines found by us are compared with the results [11]. Our ICE line intensities are normalized to the line  $L_3$  intensity 36.7 from [11]. The investigation proves existence of the 10.642-keV  $\gamma$ -transition. It follows from the analysis of the ICE line intensity ratios for this transition that it is an M1 transition; the E2 admixture  $\delta^2 \leq 0.04\%$ . Refined values were derived for the transition energies 10.642(5), 26.015(5), 36.660(5), 38.543(3), and 108.37(1) keV. Low transmission of the electrostatic spectrometer did not allow the conclusion [11] about the character of the 26.0, 36.7, and 38.5-keV  $\gamma$ -transitions to be ascertained on the basis of the ICE line intensity ratios. A more definite conclusion about the character of these transitions comes from comparison of the internal conversion coefficients ( $\alpha_L, \alpha_M$ ) derived from the experimental data with

the theoretical ones. We calculated  $\alpha_L$  and  $\alpha_M$  using the ICE line intensities from Table 4 and  $\gamma$ -ray intensities from Table 1. Note that the background from the Compton scattering of high-intensity  $\gamma$ -rays with energies  $E_\gamma > 75$  keV did not allow us to observe 26.0-keV  $\gamma$ -rays in the single  $\gamma$ -spectrum. Those  $\gamma$ -rays were only observed in coincidences with  $\alpha$ -particles in the interval  $E_\alpha \cong 5775$ -5800 keV. Based on these results and taking into account the intensity balance in the decay scheme, we found their intensities. The evaluations lead to the conclusion that the 26.0, 36.7, and 38.5-keV transitions are of E2 type with the M1 admixture no larger than 5–10%.

## IV. Discussion of the results

The decay scheme (Fig. 4) presents not only energies of  $\gamma$ -rays but also experimentally found multiplicities of transitions [11, 13, 31, 33, present paper] and total intensities of  $\gamma$ -transitions. Transition intensities were calculated with the internal conversion coefficient of the transitions whose multiplicities were determined. Intensities of the 10.6, 26.0, 36.7, and 38.5-keV transitions were calculated as a sum of ICE line intensities (see Table 4). Table 5 presents results of analyzing the balance of intensities of transitions to and from  $^{221}\text{Fr}$  levels. It is seen that for most levels the intensities of the incoming and outgoing transitions agree within the errors. For some levels populating intensities are slightly lower than de-excitation intensities. This may point to filling of these levels via low-intensity unobserved  $\gamma$ -transitions from higher levels. There is a disbalance for the 36.7-keV level noted in [11]: coming are  $(26.3 \pm 1.8)\%$ , going are  $(20.2 \pm 1.1)\%$ . The 10.6-keV  $\gamma$ -transition observed by us do not improve the situation: a disbalance of  $(6 \pm 2)\%$  remains. We assume that between the  $^{221}\text{Fr}$  ground state and 36.7-keV level there is a level a transition to which eliminates the disbalance. With this, the ground state populating intensity adds up to a value close to 100%. The energy of this level might as well be 22.3 keV. It was mentioned above that introduction of this level is not in conflict with the  $(\alpha\text{-}\gamma)$ -coincidences. In [15] existence of the 7.5, 19.0, and 50.2-keV gamma transitions was assumed to get the intensity balance. According to our data, these  $\gamma$ -transitions are not necessary to have the balance.

The  $^{221}\text{Fr}$  ground state spin and parity are  $5/2^-$ , for  $^{225}\text{Ac}$  they are probably  $(3/2^-)$  [9]. The experimental data that can be used to deter-

mine spins and parities of excited  $^{221}\text{Fr}$  states are transition multipolarities, hindrance factors of  $\alpha$ -decay (HF), relative intensities of  $\gamma$ -rays to lower-lying levels. Multipolarities of  $\gamma$ -transitions between levels (M1, E2, or E1(+M2)) allowed parities of 16 levels to be established uniquely. Experimental data for simple determining spins of the excited  $^{221}\text{Fr}$  states are insufficient. The decay scheme (Fig. 4) shows level spins predicted by calculations of Kvasil et al. [34] within the model of the axially symmetrical and reflection-asymmetrical nucleus [2] with static deformations  $\epsilon_2 = 0.10$  and  $\epsilon_3 = 0.08$ . In this case rotational bands of doublet states with  $K^\pi = 1/2^\pm$  and  $K^\pi = 3/2^\pm$  were introduced in the  $^{221}\text{Fr}$  level scheme. These spin values are not contradicted experimental data.

We calculated excitation energies and structures of low-lying nonrotational  $^{221}\text{Fr}$  states within the quasiparticle-phonon nuclear model QPNM [35, 36]. An axially symmetrical Woods-Saxon potential is used in the QPNM Hamiltonian to describe the mean field of the neutron and proton systems. Pairing, isoscalar, and isovector multipole and spin-multipole forces are taken into account as residual interaction. The odd nucleus is treated as a system comprising an even-even core and a nucleon. Calculation is carried out in the random phase approximation. Generalized phonon operators  $Q_{\mu i}$  are introduced; they have a certain projection of the momentum  $\mu$  onto the nuclear symmetry axis and comprise components with different electric and magnetic multipolarities  $\lambda$ .

Interaction of quasiparticles with phonons is taken into account for odd-A nuclei. The wave function of the ground or excited state  $K^\pi$  is written as

$$\Psi_r(K^\pi) = \frac{1}{\sqrt{2}} \sum_{\sigma} \left\{ \sum_{\rho} C_{\rho} \alpha_{\rho\sigma}^{+} + \sum_{\nu\mu i} D_{\nu\mu i} \alpha_{\nu\sigma}^{+} Q_{\mu i}^{+} \right\} \Psi_0$$

with the normalization condition

$$\sum_{\rho} C_{\rho}^2 + \sum_{\nu\mu i} D_{\nu\mu i}^2 = 1.$$

– Here  $\Psi_0$  is the quasiparticle and phonon vacuum,  $r$  is the ordinal number of the nonrotational state with the projection of the momentum  $K$  and parity  $\pi$ ,  $\sigma = \pm 1$ ,  $\rho$  or  $\nu$  is a set of quantum number of single-particle states of the mean field in terms of Nilsson representation,  $\alpha_{\rho\sigma}^{+}$  is the quasiparticle production operator,  $C_{\rho}$  and  $D_{\nu\mu i}$  are the amplitudes of

the single-quasiparticle components and quasiparticle  $\nu \otimes$  phonon  $\mu i$  components of the odd-nucleus wave function,  $i$  is the number of the phonon.

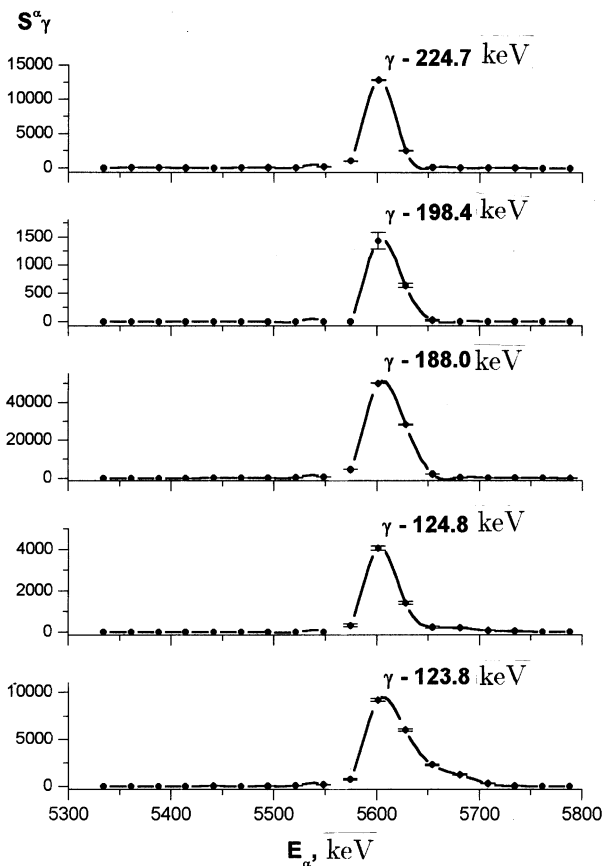
Note that in the calculation for the odd-A nucleus there are no free parameters, they are all fixed by the description of the mean field and the even-even core.

In this case the mean field is described with an axially symmetrical Woods-Saxon potential ( $A = 221$ ,  $Z = 87$ ) with the parameters from [37]. According to [38, 39],  $\beta_2 = 0.13$ ,  $\beta_4 = 0.08$ ,  $\beta_3 = 0$ . Since the  $^{225}\text{Ac}$  decay results in excitation of  $^{221}\text{Fr}$  levels with energy  $\leq 0,95$  MeV, we only dealt with states below this energy in our calculations. The calculations show that in this case it is enough to take into account residual multipole forces with  $\lambda \leq 3$  and to restrict oneself to no more than 3-5 phonons of each multipolarity. Radial dependence of these forces was taken in the form  $\partial V / \partial r$ , where  $V$  is the radial part of the mean field potential. Constants of these forces were determined as in [37, 40].

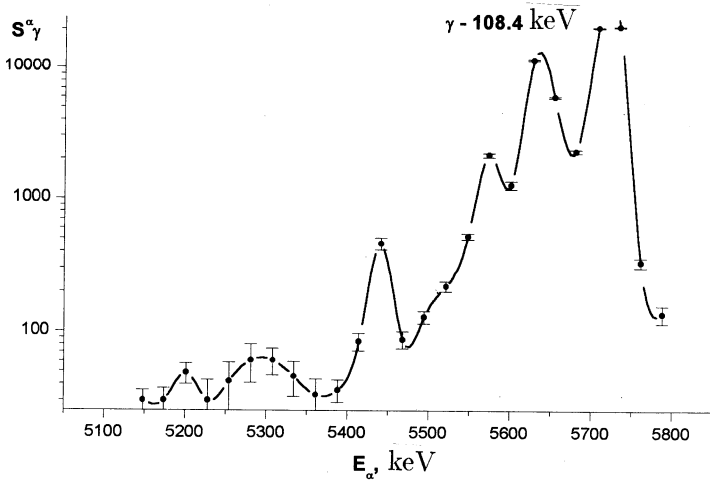
Analysis of the structure of the calculated octupole phonons showed that the anomalous decrease in energy for the region of nuclei in question might be due to presence of low-lying two-quasiparticle proton poles with large matrix elements  $f_{\nu\nu'}^{(30)}$ . The structure of these poles in terms of Nilsson representation is pp530↑660↑, pp532↓651↑, pp530↑400↑.

Table 6 presents calculated energies and structures of the lowest nonrotational states. All calculated levels up to the energy of 950 are given for each  $K^\pi$ . Comparison with the experimental results shows satisfactory agreement within the accuracy of the model (which we estimate to be within 100-300 keV). Therefore, we think that the assumption of static octupole deformation of the nuclei from the region in question needs ascertaining. It is evident from Table 6 that the lowest states for all  $K^\pi$  are close in structure to single-quasiparticle ones (the contribution from the corresponding component  $C_\rho^2$  выше 70-80% is larger than 70-80%). Among the subsequent roots for each  $K^\pi$  there are collective states of predominantly octupole type (the contribution from the components  $D_{\nu\mu i}^2$  to the wave function is as large as 80-90%). Calculations show that the structure of the higher excited states is more complicated. For example, states with  $K^\pi = 3/2^-$  have a noticeable admixture single-quasiparticle components  $3/2^-$ [532 ↓],  $3/2^-$ [521 ↑] and quasiparticle  $\otimes$  octupole phonon components  $Q_{0-1}$ .

Comparing are calculated quantum characteristics of the ground states of the lowest rotational bands with their description [34] we point



**Fig. 1** Intensity of  $(\alpha-\gamma)$ -coincidences of  $\gamma$ -rays from the 224.6-keV level as a function of the  $\alpha$ -particle energy in the window. The distributions for  $\gamma$ -123.8 and  $\gamma$ -124.8 keV are broadened on the large  $E_{\alpha}$  side because of summation of pulses from  $\alpha$ -particle and pulses from ICE of transitions from the 100.9 and 99.8-keV levels



**Fig. 2** Intensity of  $(\alpha-\gamma)$ -coincidences of 108.4-keV  $\gamma$ -rays as a function of the  $\alpha$ -particle energy

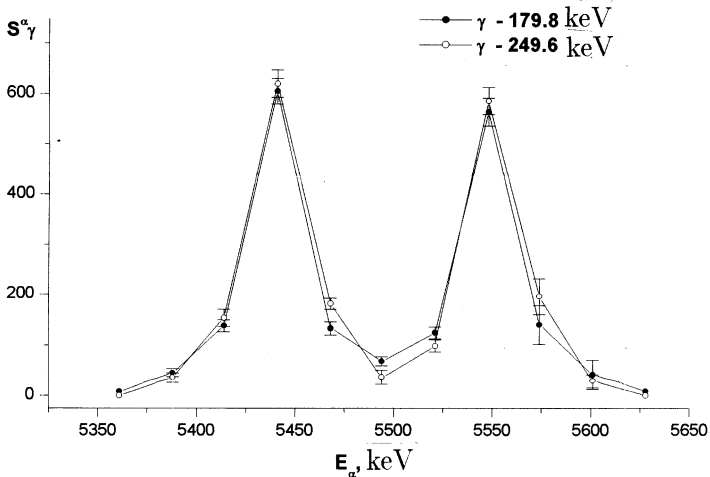


**Fig. 3** Intensity of  $(\alpha-\gamma)$ -coincidences of 179.8 and 249.7-keV  $\gamma$ -rays as a function of the  $\alpha$ -particle energy



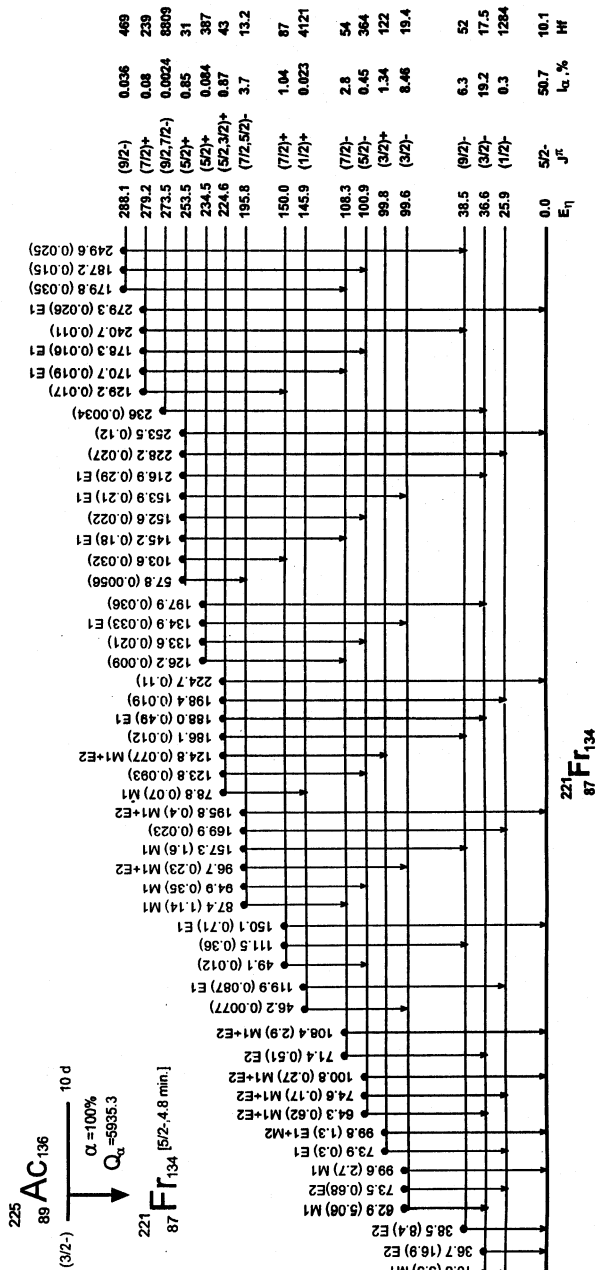


**Fig. 4**  $^{225}\text{Ac}$  decay scheme. Solid lines represent  $\gamma$ -transitions whose position is proved by the  $(\alpha-\gamma)$ -coincidences, dashed lines represent  $\gamma$ -transitions whose position is not in conflict with the  $(\alpha-\gamma)$ -coincidences. Shown above the transitions are their energies, total (including conversion) intensities (in parentheses), and experimental multipolarity data. Near the level energies there are spins, parities, intensities of the  $\alpha$ -decay to the levels, and hindrance factors.

225  
88  $AC_{136}$   
(3/2)  $\alpha = 100\%$   
 $Q_{\alpha} = 5935.3$

221  
87  $Fr_{134}$  [5/2-4.8 min.]

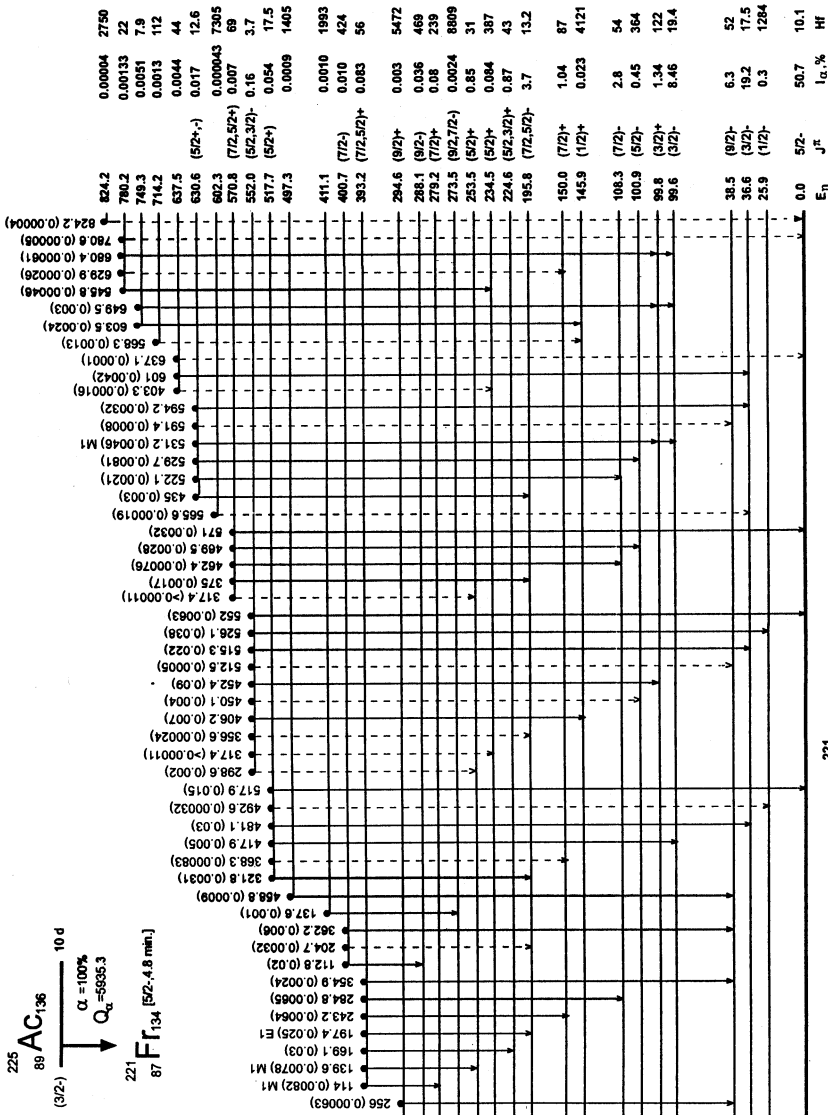


Fig. 4b.

221  $Fr_{134}$   
87

**Table 1.** Energies and intensities of the  $\gamma$ -rays in the  $^{225}\text{Ac}$  decay.

Present paper		Ardissou et al. [15]		Multipolarity	Transition placement
$E_\gamma$ , keV	$I_\gamma$ , %	$E_\gamma$ , keV	$I_\gamma$ , %	$\sigma_L$	$E_i \rightarrow E_f$
26.0	0.0015/5/ *	26.0/1/	0.00161/22/	E2(M1<60%)	25.9 $\rightarrow$ 0
36.7/1/	0.0155/14/	36.70/3/	0.0183/23/	E2(M1<20%)	36.65 $\rightarrow$ 0
38.5/1/	0.0094/8/	38.60/4/	0.0102/16/	E2(M1<20%)	38.53 $\rightarrow$ 0
46.2/2/	0.0039/6/	46.24/5/	0.0057/12/		145.9 $\rightarrow$ 99.6
49.1/2/	0.0066/7/	49.13/4/	0.0090/14/		150.0 $\rightarrow$ 100.9
-	<0.001	50.0/1/5/	<0.004		
57.8/2/	0.0039/8/	57.69/4/	0.0061/13/		253.5 $\rightarrow$ 195.8
-	-	62.6/3/	<0.03		
62.9/1/	0.43/2/	62.96/3/	0.48/6/	M1(E2<1%)	99.6 $\rightarrow$ 36.65
-	-	63.5/3/	0.021/3/		
64.3/1/	0.041/4/	64.28/3/	0.047/5/	M1+(17 $\pm$ 5)% E2	100.9 $\rightarrow$ 36.65
-	-	69.87/5/	0.0047/12/	E2(M1<35%)	
71.4/3/	0.0126/25/	71.72/4/	0.0129/14/	E2(M1<25%)	108.3 $\rightarrow$ 36.65
73.5	0.025/7/	73.36/20/	0.015/5/	E2(M1<30%)	99.6 $\rightarrow$ 25.9
73.9/1/	0.264/17/	73.85/4/	0.32/4/	E1(M2<0.1%)	99.8 $\rightarrow$ 25.9
74.6/4/	0.022/7/ *	74.82/5/	0.013/3/	M1+20% E2	100.9 $\rightarrow$ 145.9
78.6	0.0107/15/	-	-	M1*	224.6 $\rightarrow$ 25.9
87.4/1/	0.226/13/	87.42/3/	0.31/4/	M1(E2<1%), M1*	195.8 $\rightarrow$ 108.3
94.9/1/	0.084/8/	94.90/3/	0.130/19/	M1(E2<5%)	195.8 $\rightarrow$ 100.9
96.7/5/	0.028/5/	96.15/5/	<0.03	M1+(32 $\pm$ 12)% E2	195.8 $\rightarrow$ 99.6
99.6	0.70/6/	99.71/6/	1.36/19/	M1+(3 $\pm$ 1)% E2	99.6 $\rightarrow$ 0
99.8/1/	1.00/11/	100.07/10/	0.26/10/	E1(M2<0.5%)	99.8 $\rightarrow$ 0
100.8/2/	0.075/6/	100.87/4/	0.121/13/	M1+(E2)	100.9 $\rightarrow$ 0
103.6/2/	0.0023/5/	103.44/12/	0.0065/19/		253.5 $\rightarrow$ 150.0
108.4/1/	0.216/11/	108.38/3/	0.27/3/	M1+(22 $\pm$ 4)% E2	108.3 $\rightarrow$ 0
111.5/1/	0.264/14/	111.52/3/	0.34/4/		150.0 $\rightarrow$ 38.53
112.8	0.0018/2/ *	112.8/2/	<0.003		400.7 $\rightarrow$ 288.1
114	7.5/10/E-04 *	-	-	M1*	393.2 $\rightarrow$ 279.2
-	-	119.09/6/	0.018/3/		
119.9/1/	0.066/3/	119.84/3/	0.097/10/		145.9 $\rightarrow$ 25.9
-	-	121.06/7/	0.017/5/		
123.8/1/	0.072/4/	123.73/4/	0.098/10/		224.6 $\rightarrow$ 100.9
124.8/1/	0.024/1/	124.81/3/	0.032/3/	M1+E2	224.6 $\rightarrow$ 99.8
126.2/2/	0.0070/6/	126.09/5/	0.0073/14/		234.5 $\rightarrow$ 108.3
129.2/2/	0.0022/4/	129.22/7/	0.0033/11/		279.2 $\rightarrow$ 150.0
133.6/1/	0.017/1/	133.60/4/	0.096/19/		234.5 $\rightarrow$ 100.9
134.9/1/	0.027/2/	134.85/3/	0.033/5/	E1	234.5 $\rightarrow$ 99.6
137.6	0.0019/2/ *	137.40/10/	0.0030/13/		411.1 $\rightarrow$ 273.5
139.6	0.0012/2/ *	-	-	M1+(E2)*	393.2 $\rightarrow$ 253.5
144.7	0.0004/1/ *	144.7/2/	$\sim$ 0.0005	M1, M1+E2	294.6 $\rightarrow$ 150.0
145.2/1/	0.126/6/	145.15/3/	0.148/15/	E1(M2<1%), E1*	253.5 $\rightarrow$ 108.3
150.1/1/	0.60/3/	150.02/4/	0.691/16/	E1(M2<0.4%)	150.0 $\rightarrow$ 0
152.6/2/	0.019/1/	152.64/3/	0.0165/19/		253.5 $\rightarrow$ 100.9
153.9/1/	0.182/9/	153.91/3/	0.195/20/	E1*	253.5 $\rightarrow$ 99.6
157.3/2/	0.32/2/	157.24/3/	0.35/4/	M1(E2<4%)	195.8 $\rightarrow$ 38.53
-	-	161.35/7/	0.0036/9/		
169.1	0.007/1/ *	169.18/4/	0.0158/19/		393.2 $\rightarrow$ 224.6
169.9	0.012/1/ *	-	-		195.8 $\rightarrow$ 25.9
170.7/2/	0.017/1/	170.83/6/	0.0073/13/	E1	279.2 $\rightarrow$ 108.3

173.4	0.010/1/	-	-		°
178.3/2/	0.014/1/	178.29/3/	0.0160/18/	E1	279.2 → 100.9
179.8/3/	0.0094/6/	179.78/4/	0.0106/13/		288.1 → 108.3
183	0.0073/11/	-	-		°
186.1	0.0111/1/ *	-	-		224.6 → 38.53
186.3	0.0036/3/ *	186.31/3/	0.0189/21/	E1	294.6 → 108.3
187.2	0.0089/3/ *	-	-		288.1 → 100.9
188.0/1/	0.45/2/	187.95/3/	0.54/6/	E1(M2<0.5%)	224.6 → 36.65
193.2	0.0017/3/	-	-		°
195.8/2/	0.123/6/	195.74/3/	0.162/16/	M1+(40±20)% E2	195.8 → 0
197.4	0.023/2/ *	197.50/3/	0.054/7/	E1*	393.2 → 195.8
197.9	0.033/3/ *	-	-		234.5 → 36.65
198.4/3/	0.017/1/	198.23/8/	0.0176/18/		224.6 → 25.9
204.7/3/	0.0011/4/	205.12/11/	0.0019/7/		(400.7 → 195.8)
216.9/2/	0.271/14/	216.89/3/	0.33/3/		253.5 → 36.65
-	-	220.43/8/	0.0060/18/		
224.7/1/	0.098/5/	224.58/3/	0.108/12/		224.6 → 0
228.2/4/	0.004/1/	-	-		253.5 → 25.9
231.3/2/	0.0066/6/	231.14/7/	0.0021/5/		°
236.0/6/	0.0015/2/	-	-		273.5 → 36.65
-	-	238.64/8/	0.0010/3/		
240.7/2/	0.010/1/	240.68/3/	0.0118/13/		279.2 → 38.53
243.2/2/	0.0030/3/	243.11/5/	0.0027/5/		393.2 → 150.0
249.6/2/	0.012/1/	249.60/3/	0.0131/14/		288.1 → 38.53
253.5/1/	0.116/6/	253.45/3/	0.128/13/		253.5 → 0
256	0.0006/2/ *	256.0/2/	0.00032/10/		294.6 → 38.53
279.3/3/	0.025/2/	279.18/3/	0.032/3/	E1	279.2 → 0
284.8/3/	0.0063/5/	284.75/3/	0.0075/9/		393.2 → 108.3
298.6/3/	0.0018/5/	298.32/5/	0.0020/3/		(552.0 → 253.5)
317.4	>0.00011/5/ *	317.23/18/	0.00042/21/		552.1 → 234.5
					570.8 → 253.5
321.8/4/	0.0030/4/	321.77/4/	0.0032/5/		517.7 → 195.8
348.2/4/	0.0025/3/	348.33/4/	0.0032/5/		°
354.9/3/	0.0023/3/	354.54/6/	0.00128/23/		393.2 → 38.53
356.6	2.2/9/E-04 *	-	-		(552.0 → 195.8)
362.2/4/	0.0042/4/	362.38/3/	0.0062/7/		400.7 → 38.53
368.3/6/	0.0006/2/	367.72/12/	<0.03		(517.7 → 150.0)
375.0/7/	0.0017/4/	374.98/5/	0.00019/3/		570.8 → 195.8
-	-	388.07/7/	0.00121/23/		
403.4/3/	0.00016/14/	403.1/1/	<0.002		(637.5 → 234.46)
406.2/3/	0.0067/4/	405.95/3/	0.0079/9/		552.0 → 145.9
417.9/3/	0.0048/4/	417.90/3/	0.0057/7/		517.7 → 99.6
-	-	429.80/18/	0.00038/19/		
435.0/3/	0.0024/3/	434.81/5/	0.0032/5/		630.6 → 195.8
-	-	442.16/8/	0.0045/7/		
-	-	443.43/10/	0.0014/5/		
-	-	446.31/10/	0.0006/3/		
450.1/7/	0.0032/8/	451.04/5/	0.0028/5/		(552.0 → 100.9)
452.4/2/	0.089/5/	452.21/3/	0.118/13/		552.0 → 99.8
458.8/4/	5.8/22/E-04	458.78/8/	0.00045/11/		(497.3 → 38.53)
462.4/6/	7.5/27/E-04	462.43/13/	0.00038/11/		570.8 → 108.3
469.5/3/	0.0028/3/	469.48/5/	0.0018/7/		570.8 → 100.9
481.1/2/	0.029/2/	480.84/3/	0.034/4/		517.7 → 36.65
492.6/6/	0.00022/14/	491.42/10/	0.00039/12/		(517.7 → 25.9)

498.6/6/	0.0007/2/	-	-	(815 → 316)
512.5/7/	0.0005/2/	-	-	(552.0 → 38.53)
515.3/2/	0.019/1/	515.12/3/	0.0204/21/	552.0 → 36.65
517.9/2/	0.015/1/	517.50/3/	0.0145/15/	517.7 → 0
522.1/2/	0.0018/3/	522.14/4/	0.00205/24/	630.6 → 108.3
526.1/1/	0.033/2/	525.77/3/	0.032/3/	552.0 → 25.9
-	-	527.29/5/	0.0019/3/	
529.7/3/	0.0071/7/	529.59/3/	0.0070/8/	630.6 → 100.9
531.2/3/	0.0040/5/	530.86/4/	0.0047/6/	630.6 → 99.6/99.8
-	-	532.11/9/ *	0.00073/19/	
545.8/6/	0.00046/12/	-	-	780.2 → 234.5
552.0/2/	0.0056/4/	551.78/3/	0.0039/5/	552.0 → 0
565.6/7/	0.00019/8/	564.31/11/	~0.0001	(602.3 → 36.65)
568.3/6/	0.0013/3/	567.47/5/	0.00093/13/	(714.2 → 145.9)
571.0/2/	0.0032/5/	570.68/3/	0.0041/5/	570.8 → 0
591.4/7/	0.0007/2/	590.41/5/	0.00084/14/	(630.6 → 38.53)
594.6/3/	0.0028/6/	593.86/4/	0.0028/3/	630.6 → 36.65
601.0/3/	0.0037/9/	600.92/3/	~0.008	637.5 → 36.65
603.5/5/	0.0016/4/	603.09/4/	0.00170/21/	749.3 → 145.9
629.9/7/	0.00026/8/	628.93/10/	0.00034/9/	(780.2 → 150.0)
637.1/7/	~0.0001	-	-	(637.5 → 0)
646.3/3/	0.00010/4/	645.87/13/	0.00022/7/	
649.5/2/	0.0012/3/	649.01/4/	0.00185/22/	749.3 → 99.8/99.6
653.5/4/	0.00015/4/	-	-	
-	-	656.18/11/	0.00049/23/	
-	-	657.88/5/	0.0014/3/	
668.1/4/	0.00024/7/	667.10/8/	0.0039/9/	
674.3/4/	0.00007/4/	675.51/18/	0.00013/6/	
680.4/6/	0.00061/15/	679.35/6/	0.00062/12/	780.2 → 99.8/99.6
698.4/4/	0.00017/5/	697.54/13/	0.00024/9/	
-	-	702.00/14/	0.00016/7/	
747	<0.0001	747.0/1/	<0.002	
-	-	752.46/12/	0.00026/7/	
753.7	<0.0001	754.04/13/	0.00023/7/	
768.4/5/	0.00024/7/	767.6/4/	0.00034/9/	
780.6/6/	0.00005/1/	-	-	(780.2 → 0)
-	-	808.48/10/	0.0021/3/	
824.2/7/	~0.00004	-	-	(824.2 → 0)

<sup>a</sup> –  $\gamma$ -ray intensity determined from ( $\alpha$ - $\gamma$ )-coincidence;

<sup>c</sup> –  $\gamma$ -rays, ascribing of which to <sup>225</sup>Ac decay is doubtful;

\* –  $\sigma_L$  established in present paper.

**Table 2.** Population of the  $^{221}\text{Fr}$  levels by the  $^{225}\text{Ac}$  alpha-decay..

E <sub>level</sub> , кэВ	Present paper			a <sub>ci</sub> , % [9]	Hf
	a <sub>ci</sub> /a <sub>i</sub>	a <sub>i</sub> , %	a <sub>ci</sub> , %		
36.65	0.95/7/	20.2/11/	19.15/176/	18.1/20/	17.5/16/
38.53	0.75/8/	8.4/5/	6.3/8/	8.6/9/	52/7/
99.6	0.995/71/	8.5/4/	8.5/7/	8.0/1/	19.4/17/
99.8	0.84/2/	1.6/2/	1.34/17/	1.32/10/	122/16/
100.9	0.43/2/	1.05/8/	0.45/4/	0.87/23/	364/32/
108.3	0.73/1/	3.77/19/	2.77/15/	3.1	54/3/
145.8	0.24/1/	0.095/4/	0.023/2/	-	4121/253/
150	0.96/1/	1.08/5/	1.04/5/	1.3/2/	87/4/
195.8	1.00/2/	3.7/1/	3.7/1/	4.4/3/	13.2/4/
224.6	1.01/4/	0.86/3/	0.87/5/	1.1/1/	43/3/
234.5	0.85/1/	0.099/4/	0.084/4/	0.04	387/18/
253.5	0.95/2/	0.89/3/	0.85/3/	1.2/1/	31/1/
273.5	0.69/29/	0.0034/5/	0.0024/10/	0.034	8809/3670/
279.2	0.89/2/	0.089/4/	0.079/4/	0.1	239/12/
288.1	0.48/3/	0.075/3/	0.036/3/	0.03/1/	469/39/
294.6	0.41/2/	0.0070/7/	0.0029/3/	0.015	5472/566/
393.2	0.96/7/	0.086/4/	0.083/7/	0.14/1/	56/5/
400.7	0.35/14/	0.029/2/	0.010/5/	0.07/2/	424/212/
411.1	-	0.0010/1/	0.0010/1/*	<0.003	1993
497.3	-	0.0009/3/	0.0009/3/*	<0.001	1405/877/
517.7	0.99/3/	0.054/2/	0.054/3/	0.07/1/	17.5/10/
552	0.91/3/	0.17/1/	0.16/1/	0.23/1/	3.7/2/
570.8	0.80/7/	0.0086/8/	0.0069/9/	0.014/5/	69.2/90/
602.3	0.23/20/	0.00019/8/	0.000043/32/	0.0030/8/	7305/5436/
630.6	0.77/9/	0.022/2/	0.017/2/	0.030/3/	12.6/17/
637.5	-	0.0044/6/	0.0044/6/*	0.0020/5/	43/6/
714.2	-	0.0013/3/	0.0013/3/*	0.0020/8/	112
749.3	0.94/8/	0.0054/15/	0.0051/15/	0.006/1/	7.9/23/
780.2	0.95/9/	0.0014/2/	0.00133/23/	0.003/1/	21/4/
824.2	-	~0.00004	~0.00004*	<0.001	2750

\* - a<sub>ci</sub>/a<sub>i</sub> - are not determined in (α-γ)-coincidences; used a<sub>ci</sub> - obtained from intensities balance.

**Table 3.** Determination of  $\gamma$ -transition multiplicities from total internal conversion coefficients.

$E_{\gamma i}$ , keV	$E_p \rightarrow E_i$	$S_{\gamma ik}^{ap}/S_{\gamma ik}^{ai}$	$a_{\gamma i}$	$\alpha_{\gamma i}$ experiment	$\alpha_{\gamma i}$ calculate	$\sigma_L$
78.8	224.6 $\rightarrow$ 145.9	2.8/2/	0.065/8/	5.1/11/	0.19 (E1) 25.5 (E2) 5.3 (M1)	M1
87.4	195.8 $\rightarrow$ 108.3	0.31/4/	0.86/12/	2.8/6/	0.15 (E1) 15.6 (E2) 4.2 (M1)	M1
114	393.2 $\rightarrow$ 279.2	0.14/1/	0.0105/13/	13.0/17/	0.34 (E1) 4.8 (E2) 9.9 (M1)	M1
139.6	393.2 $\rightarrow$ 253.5	0.0061/6/	0.0050/6/	3.2/5/	0.21 (E1) 2.1 (E2) 5.5 (M1)	M1(+E2)
145.2	253.5 $\rightarrow$ 108.3	0.043/9/	0.11/3/	$\leq 0.1$	0.19 (E1) 1.77 (E2) 5 (M1)	E1
153.9	253.5 $\rightarrow$ 99.6	0.025/5/	0.20/4/	$\leq 0.35$	0.17 (E1) 1.4 (E2) 4.2 (M1)	E1
197.4	393.2 $\rightarrow$ 195.8	0.0062/2/	0.022/2/	$\leq 0.04$	0.09 (E1) 0.55 (E2) 2.1 (M1)	E1

**Table 4.** Energies and intensities of ICE lines in the  $^{225}\text{Ac}$  decay ( $E_c < 25$  keV).

Line	Present paper		Dzhelepov et al. [11]	
	$E_c$ , keV	$I_c$	$I_c$	$\sigma_L$
$E_\gamma = 10.642/5/$ keV				
M <sub>1</sub>	5.997/2/	2.20/13/	-	
M <sub>2</sub>	6.324/6/	0.28/6/	-	
M <sub>3</sub>	-	<0.15 (95% C.L.)	-	
N <sub>1</sub>	9.501/3/	0.78/6/	-	
$E_\gamma = 26.015/5/$ keV				
L <sub>2</sub>	8.112/4/	2.72/16/	-	
L <sub>3</sub>	10.992/3/	2.68/7/	-	
M <sub>2</sub>	21.705/8/	1.00/25/	-	
M <sub>3</sub>	22.366/7/	1.22/26/	0.9/1/	E2+(M1<60%)
$E_\gamma = 36.660/5/$ keV				
L <sub>2</sub>	18.757/4/	5.69/23/	6.1/7/	E2+(M1<20%)
L <sub>3</sub>	21.636/3/	6.20/29/	6.2/8/	
$E_\gamma = 38.543/3/$ keV				
L <sub>2</sub>	20.641/3/	3.07/17/	3.1/3/	E2+(M1<20%)
L <sub>3</sub>	23.518/3/	3.66/32/	3.1/4/	
$E_\gamma = 108.37/1/$ keV				
K	7.242/8/	1.19/10/	-	M1+22%E2

**Table 5.** Intensity balance for  $^{221}\text{Fr}$  levels at the  $^{225}\text{Ac}$  decay.

Level $E_{\eta}$ , keV	Populate			Unload $a_{\gamma+e}$ , %
	$a_{\alpha}$ , %	$a_{\gamma+e}$ , %	$a_{\alpha+\gamma+e}$ , %	
0	50.7/15/*	42/2/	93/2/	
25.9	0.3*	4.7/2/	5.3/2/	7.6/14/
36.65	19.15/176/	7.1/3/	26.3/18/	20.2/11/
38.53	6.3/8/	2.34/12/	8.6/8/	8.4/5/
99.6	8.5/7/	0.49/4/	8.9/7/	8.5/4/
99.8	1.34/17/	0.17/1/	1.5/2/	1.6/2/
100.9	0.45/4/	0.54/3/	0.99/5/	1.05/8/
108.3	2.77/15/	1.3/1/	4.2/2/	3.8/2/
145.9	0.023/2/	0.08/1/	0.10/2/	0.095/4/
150	1.04/5/	0.06/1/	1.1/1/	1.08/5/
195.8	3.7/1/	0.042/3/	3.7/1/	3.7/1/
224.6	0.87/5/	0.029/3/	0.9/1/	0.86/3/
234.5	0.084/4/	0.0006/2/	0.085/4/	0.099/4/
253.5	0.85/3/	0.0097/14/	0.86/3/	0.89/3/
273.5	0.0024/10/	>0.0010/1/	>0.0034/10/	0.0034/5/
279.2	0.079/4/	0.008/1/	0.087/4/	0.089/4/
288.1	0.036/3/	>0.020/2/	0.056/4/	0.075/3/
294.6	0.0029/3/		0.0029/3/	0.0070/7/
393.2	0.083/7/		0.083/7/	0.086/4/
400.7	0.010/5/		0.010/5/	0.029/2/
411.1	<0.003*		<0.003	0.0010/1/
497.3	<0.001*		<0.001	0.0009/3/
517.7	0.054/3/		0.054/3/	0.054/2/
552	0.16/1/		0.16/1/	0.17/1/
570.8	0.0069/9/		0.007/1/	0.0086/8/
602.3	0.000043/32/		0.000043/32/	0.00019/8/
630.6	0.017/2/		0.017/2/	0.022/2/
637.5	0.0020/5/*		0.0020/5/	0.0044/6/
714.2	0.0020/8/*		0.0020/8/	0.0013/3/
749.3	0.0051/15/		0.0051/15/	0.0054/15/
780.2	0.00133/23/		0.0013/2/	0.0014/2/
824.2	<0.001*		<0.001	~0.00004

\* - value of  $a_{\alpha}$  (%) taken from [9].



**Table 6.** Energy (experimental and teoretical (QPNM), in keV) and structure of the lowest nonrotational states of  $^{221}\text{Fr}$

N	$E, I^\pi$	$K_r^\pi$	$E$	$(C_\rho^2 + D_{\nu\mu i}^2)$
1	<b>25.9(1/2)<sup>-</sup></b>	$1/2_1^-$	0	530↑ (86%) + 651↑ $\otimes Q_{1-}^1$ (4%)
		$1/2_2^-$	490	541↓ (79%) + 660↑ $\otimes Q_{0-}^1$ (14%)
		$1/2_3^-$	630	541↓ (14%) + 660↑ $\otimes Q_{0-}^1$ (81%)
		$1/2_4^-$	850	541↓ (3%) + 660↑ $\otimes Q_{1-}^1$ (96%)
2	<b>36.6(3/2)<sup>-</sup></b> <b>552(5/2, 3/2)<sup>-</sup></b>	$3/2_1^-$	80	532↓ (89%) + 651↑ $\otimes Q_{0-}^1$ (4%)
		$3/2_2^-$	410	521↑ (66%) + 651↑ $\otimes Q_{0-}^1$ (13%)
		$3/2_3^-$	850	521↑ (1%) + 660↑ $\otimes Q_{1-}^1$ (97%)
3	<b>145.9(1/2)<sup>+</sup></b>	$1/2_1^+$	120	660↑ (93%) + 530↑ $\otimes Q_{0-}^1$ (2%)
		$1/2_2^+$	740	400↑ (54%) + 541↓ $\otimes Q_{0-}^1$ (33%)
		$1/2_3^+$	890	400↑ (20%) + 541↓ $\otimes Q_{0-}^1$ (37%)
		$1/2_4^+$	950	400↑ (9%) + 530↑ $\otimes Q_{0-}^1$ (63%)
4	<b>224.6(5/2, 3/2)<sup>+</sup></b>	$3/2_1^+$	200	651↑ (77%) + 530↑ $\otimes Q_{1-}^1$ (8%)
		$3/2_2^+$	830	402↓ (12%) + 532↓ $\otimes Q_{0-}^1$ (79%)
		$3/2_3^+$	940	402↓ (59%) + 400↑ $\otimes Q_{2+}^1$ (16%)
5	<b>517.7(5/2)<sup>+</sup></b>	$5/2_1^+$	530	642↑ (74%) + 521↑ $\otimes Q_{1-}^1$ (6%)
6	<b>630.6(5/2<sup>±</sup>)</b>	$5/2_1^-$	480	523↓ (90%) + 642↑ $\otimes Q_{0-}^1$ (4%)
7		$7/2_1^+$	780	633↑ (77%) + 651↑ $\otimes Q_{2+}^1$ (6%)

out that parities of well-identified states coincided in all cases in both approaches. As to the views of their quasiparticle structure, they are different in most cases. This is probably due to the use of different mean field potentials in the two approaches and the presence of static octupole deformation in [34]. We shall refine parameters of the Woods-Saxon potential while performing calculations for other nuclei from the region of A in question, but the energy position of the lowest single-particle levels may change but very slightly. For example, according to our calculations, the  $5/2^+ [402 \uparrow]$  single-particle level lies much lower in the potential well than it is in [34], where this level characterizes the  $5/2^+$  rotational band with the ground state energy 517.51 keV.

#### Referens

1. F. Stephens, F. Asaro, I. Perlman. // Phys. Rev., 1954. V.96. P.1568; 1954. V.100. P.1543.  
P.B. Firestone, V.S. Shirley. //Table of Isotopes, 1996. eighth edition.
2. G.A. Leander et al.// Nucl. Phys., 1982. A388. P.452; 1984. A413. P.375.
3. R.V. Jolos et al. // Journ. Phys. G: Nucl. Phys., 1993. V.19, P.151.
4. V.G. Soloviev. Theory of Complex Nuclei (in russian). Moskow. Nauka, 1971;  
L.A.Malov, V.G. Soloviev, P. Vogel. //Phys. Lett., 1966. V.22. P.441.
5. K. Neergard, P. Vogel. //Nucl. Phys., 1970. A149, P.209, 217.
6. R.V. Jolos, Yu.V. Palchikov, V.V. Pashkevich et al.// Nuov. Cim., 1997. A110. P.941.
7. B.S. Dzhelepov, R.B. Ivanov, M.A. Mikhailova et al.,// Izv. AN SSSR. ser.fiz., 1967. V.31, P.568.
8. G. Bastin-Scoffier. // Comp. Rend., 1967. B265. P.863.
9. Y.A. Akovali. // Nucl. Data Sheets, 1990. V.61, P.623.
10. C.F. Liang. Compt. Rend. 1967. B.265. P.147.

11. B. S. Dzhelepov, R.B. Ivanov, M.A. Mikhailova et al. // *Izv. AN SSSR ser. fiz.*, 1972. V.36. P.2079.
12. J.K. Dickens, J.W. McConnell. // *Radiochem. Radioanal. Lett.*, 1981. V.47. P.331.
13. M.C. Kouassi, J. Dalmasso, H. Maria et al. // *J.Radional. Nucl. Chem. Letters*, 1990. V.144. P.387.
14. M.C. Kouassi, J. Dalmasso, M. Hussonois et al. // *J.Radional. Nucl. Chem. Letters*, 1991. V.153. P.293.
15. G. Ardisson, R.K. Sheline et al. // *Phys. Rev. C*, 2000. V.62, 064306.
16. B.S. Dzhelepov, A.V. Zolotavin, R.B. Ivanov et al. // *Izv. AN SSSR, ser.fiz.*, 1969. V.33. P.1607.
17. E.A. Jakushev et al. // *J. Phys. G: Nucl. Part. Phys.*, 2002. V.28. P.463.
18. C.F. Liang, A. Peghaire, R.K. Sheline. // *Modern Phys. Lett., A*. 1990. V.5. P.1243.
19. A. Peghaire. // *Ph.D. Thesis. Universite de Paris-Sud*, 1977.
20. K.Ya. Gromov, M.Ya. Kuznetsova, Yu.V. Norseev et al.// *Izv. RAN, ser.fiz.*, 1994. V.58. P.35.
21. V.I. Fominykh, J. Wawryszczuk, G.V. Veselov et al. // *Pribory i Tekhnika Experimenta (in russian)*, 1995. V.38. No 5, Part 1, P.572
22. V.V. Tsupko-Sitnikov, Yu.V. Norseev, V.A. Khalkin. // *Journal of Radioanal. Nucl. Chem.*, 1996. V.202, P.75.
23. K.Ya. Gromov, D.K. Dzhabber, Sh.R.Malikov et al. // *Izv. RAN, ser.fiz.*, 1999. V.63. No 5. P.860.
24. V.G. Chumin, V.I. Fominykh, K.Ya. Gromov et al. // *Z. Phys.*, 1997. A358 P.33.
25. V.G. Chumin, S.S. Eliseev, K.Ya. Gromov et al. // *Izv. RAN ser.fiz.*, 1995. V.59.No 11. P.58.
26. V.G. Chumin, D.K. Dzhabber, K.V. Kalyapkin et al.. // *Izv. RAN ser.fiz.*, 1997. V.61. No 11. P.2062.
27. K.Ya. Gromov, S.A. Kudrya, Sh.R. Malikov et al. // *Izv. RAN. ser. fiz.* 2000. V 64, P 2228.
28. K.Ya. Gromov, S.A. Kudrya, Sh.R. Malikov et al. // *The Book of Abstracts "LI Meeting on Nuclear Spectroscopy and Nuclear Structure"*, 3-8 September 2001, Sarov, P.179.

29. K.Ya. Dromov, V.I. Fominykh. // *Izv. RAN ser.fiz.*, 1997. V.61, No 11, P.2051.
30. I.M. Band, M.B. Trzhaskovskaya. // *Tables of  $\gamma$ -ray on internal conversion coefficients (in russian)*. 1978. Leningrad.
31. B.S. Dzhelepov, A.V. Zolotavin, R.B. Ivanov et al. // *Izv. AN SSSR ser.fiz.*, 1970. V.34, P.2127.
32. N.A. Golovkov, B.S. Dzhelepov, R.B. Ivanov et al. // *Yadernaya Fizika*, 1972. V.15. P.629.
33. Ts. Vylov, N.A. Golovkov, B.S. Dzhelepov et al. // *Izv. AN SSSR ser.fiz.*, 1977. V.41. P.1634.
34. J.Kvasil.// *Int. J. Mod. Phys.*, 1992. E1. P.845.
35. V.G. Soloviev.// *Theory of Atomic Nucleus, Quasiparticles and Phonons, (in russian)*. Moskwa. 1989.  
V.G. Soloviev, A.V. Sushkov, N.Yu. Shirikova.// *EChAYa (in russian)*. 1994. V.25.,P.377.
36. L.A. Malov.// *Izv.RAN ser.fiz.* 1996. V. 60. P.47.  
L.A. Malov.// *Izv.RAN ser.fiz.* 1996. V. 62. P.887
37. L.A. Malov, V.G. Soloviev.// *EChAYa (in russian)*. 1980. V.11. P.301.
38. Löbner K.E.G. et al.// *Nucl. Data Tabl.* 1970. A7. P. 495.
39. S.P. Ivanova et al.// *Communication of the JINR.* 1974. R4-8406. Dubna.
40. D.G. Burke D.G. et al.// *Nucl.Phys.* 1999. A656. P.287.

Received on August 28, 2002.

Кудря С. А. и др.  
Альфа-распад  $^{225}\text{Ac} \rightarrow ^{221}\text{Fr}$

E6-2002-202

Выполнено детальное исследование ( $\alpha$ - $\gamma$ )-совпадений при распаде  $^{225}\text{Ac}$ . Обнаружен 21 новый слабый  $\gamma$ -переход; восемнадцать  $\gamma$ -переходов, ранее описанных распаду  $^{225}\text{Ac}$ , не подтверждены. Количественный анализ ( $\alpha$ - $\gamma$ )-совпадений позволил определить интенсивности заселения уровней  $^{221}\text{Fr}$   $\alpha$ -распадом и мультипольности пяти слабых  $\gamma$ -переходов. Исследован спектр конверсионных электронов в диапазоне 5 + 24 кэВ при высоком ( $\sim 20$  эВ) энергетическом разрешении. Обнаружен новый  $\gamma$ -переход с энергией 10,6 кэВ типа M1. Предлагаемая схема распада  $^{225}\text{Ac}$  включает в себя 31 возбужденное состояние  $^{221}\text{Fr}$ . Для 16-ти из них установлены четности. Предлагаются возможные значения спина уровней  $^{221}\text{Fr}$ . Свойства возбужденных состояний  $^{221}\text{Fr}$  удовлетворительно описываются квазичастично-фононной моделью ядра без предположения о наличии статической октупольной деформации.

Работа выполнена в Лаборатории ядерных проблем им. В. П. Джелепова ОИЯИ.

Препринт Объединенного института ядерных исследований. Дубна, 2002

Kudrya S. A. et al.  
Alpha Decay  $^{225}\text{Ac} \rightarrow ^{221}\text{Fr}$

E6-2002-202

In-depth investigation of ( $\alpha$ - $\gamma$ )-coincidences at the  $^{225}\text{Ac}$  decay is carried out. Twenty-one new weak  $\gamma$ -rays are found; 18  $\gamma$ -rays earlier ascribed to the  $^{225}\text{Ac}$  decay are not confirmed. The quantitative analysis of the ( $\alpha$ - $\gamma$ )-coincidences makes it possible to find the intensity of population of  $^{221}\text{Fr}$  levels by the  $\alpha$  decay and multipolarities of five weak  $\gamma$ -transitions. The conversion electron spectrum is investigated in the range of 5 + 24 keV with a high (some 20 eV) energy resolution. A new M1 type 10.6-keV  $\gamma$ -transition is found. The proposed  $^{225}\text{Ac}$  decay scheme includes 31 excited  $^{221}\text{Fr}$  states. Parities are established for 16 of them. Possible spin values are proposed for  $^{221}\text{Fr}$  levels. Properties of excited  $^{221}\text{Fr}$  states are satisfactorily described by the quasiparticle-phonon nuclear model without the assumption of static octupole deformation.

The investigation has been performed at the Dzhelupov Laboratory of Nuclear Problems, JINR.

Preprint of the Joint Institute for Nuclear Research. Dubna, 2002

*Макет Т. Е. Попеко*

Подписано в печать 04.10.2002.

Формат 60 × 90/16. Бумага офсетная. Печать офсетная.

Усл. печ. л. 1,93. Уч.-изд. л. 2,14. Тираж 320 экз. Заказ № 53548.

Издательский отдел Объединенного института ядерных исследований  
141980, г. Дубна, Московская обл., ул. Жолио-Кюри, 6.